AN INTEGRATED THERMOELASTIC ANALYSIS FOR PERIODICALLY LOADED SPACE STRUCTURES

O. Rand * D. Givoli *
Department of Aerospace Engineering
Technion — Israel Institute of Technology
Haifa 32000, Israel

Abstract

An integrated thermoelastic analysis of space structures in periodic motion is performed. To this end, a combined spectral-finite-element method is devised. The thermal problem is strongly nonlinear due to the presence of heat radiation. Any symmetry which the structure may possess with respect to the axis of rotation is exploited in the numerical scheme, and leads to saving in computational cost. A numerical example is presented which demonstrates the performance of the method and its ability to identify some key characteristics in space structure problems.

Introduction

In the last few years, much attention has been given to the thermal and structural design and analysis of large space structures. Typically, these are three dimensional truss-type structures which are exposed to thermal loading in the form of solar radiation, infra-red planetary radiation and planetary albedo (solar radiation reflected from planets). Finding the spatial and temporal variation of the temperature field in the structure resulting from this radiation is important for the thermal design. In addition, the dynamic temperature field may also give rise to the dynamic deformation of the structure. This deformation is of interest due to the limitations on the allowed magnitude of the deflection of instruments and antennas, and due to the necessity to avoid a resonance.

The periodicity in the thermal loading may originate, for example, from the repetitive orbit of the space-structure around the earth or from the spinning of the structure itself. The problem is strongly nonlinear owing to the presence of heat radiation. A further complication is sometimes introduced when part of the structure overshadows another part of it during the motion. For a discussion on the factors involved in this type of analysis see refs. 1–4.

In this paper, a method is proposed for the thermal and elastic analyses of space structures in periodic motion. This method is based upon the concept developed in Rand and Givoli[5], i.e. the combination of finite elements to discretize space, and Fourier series to represent time variations. The coefficients of the Fourier series representing the solution variables are the unknowns in the formulation. The process of determining them is coded symbolically in the computer program itself, a feature which saves a lot of complicated manual calculations, and enables the easy treatment of the nonlinear terms. The treatment of time is thus analytic in nature, and time-stepping is totally avoided.

Finite Element Formulation

Consider a three-dimensional truss exposed to a time-periodic incoming heat flux. Each truss member emits radiation to space. The usually weak effect of heat exchange through radiation between different truss members is neglected. Also, the members are assumed to be slender, so that variation of temperature within the cross-section may be neglected. The governing equation is

$$\rho c \frac{\partial \mathcal{T}}{\partial t} = \frac{\partial}{\partial s}\left(k \frac{\partial \mathcal{T}}{\partial s}\right) - C_R \mathcal{T}^4 + q \ , \quad \text{in each} \quad \Omega_m . \qquad (1)$$

Here Ω_m is the mth truss member ($m = 1, ..., N_{mem}$), t is time, s is the axial coordinate along Ω_m, $\mathcal{T}(s,t)$ is the temperature, ρ is the mass density, c is the specific heat, k is the conductivity, q is a given time-periodic incident flux, and C_R is the radiation coefficient given by

$$C_R = \sigma \epsilon \frac{p}{A} \ . \qquad (2)$$

Here σ is the universal Stefan-Boltzmann constant, ϵ is the surface emissivity of the truss member, p is the perimeter of the member's cross-section, and A is the cross-sectional area.

A dot and a prime over a variable will be used to indicate differentiation with respect to time and with respect to s, respectively. Now the Galerkin finite element method is used to approximate the variational counterpart of (1) involving an arbitrary weighting function $w(s)$. To this end

* Assistant Professor, Aerospace Engineering

the spatial domain is discretized into elements. The domain of element e is denoted by Ω^e. It is important to note that each truss member Ω_m in itself is decomposed into finite elements. This is necessary due to the *nonlinear* character of the problem. In each element the functions $\mathcal{T}$ and w are approximated by

$$\begin{aligned} \mathcal{T}^h(s,t) &= \sum_{a=1}^{N_{en}} T_a(t)\, N_a(s), \\ w^h(s) &= \sum_{a=1}^{N_{en}} c_a\, N_a(s). \end{aligned} \tag{3}$$

Here N_{en} is the number of nodes of the element, N_a is the element shape function associated with node number a, T_a is the temperature at node a, and each c_a is a constant. Now using the expansions (3) in the variational form of (1) and noting that the equation that results must be true for any combination of constants c_a, leads to the following semi-discrete system of equations:

$$\boldsymbol{G}\dot{\boldsymbol{T}} + \boldsymbol{P}\boldsymbol{T} + \boldsymbol{R}(\boldsymbol{T}) = \boldsymbol{Q}\ . \tag{4}$$

$\boldsymbol{G}$ is the capacity matrix, $\boldsymbol{P}$ is the conductivity matrix, $\boldsymbol{R}$ is the radiation vector, $\boldsymbol{Q}$ is the thermal load vector, and $\boldsymbol{T}$ is the temperature vector, which contains the unknown temperatures at the nodes. These matrices and vectors are obtained by

$$\begin{aligned} \boldsymbol{G} &= \mathcal{A}_{e=1}^{N_{el}} \boldsymbol{g}^e \quad ; \quad \boldsymbol{P} = \mathcal{A}_{e=1}^{N_{el}} \boldsymbol{p}^e \quad ; \\ \boldsymbol{R} &= \mathcal{A}_{e=1}^{N_{el}} \boldsymbol{r}^e \quad ; \quad \boldsymbol{Q} = \mathcal{A}_{e=1}^{N_{el}} \boldsymbol{q}^e \quad ; \\ \boldsymbol{g}^e &= [g_{ab}^e] \quad ; \quad \boldsymbol{p}^e = [p_{ab}^e] \quad ; \\ \boldsymbol{r}^e &= \{r_a^e\} \quad ; \quad \boldsymbol{q}^e = \{q_a^e\} \quad . \end{aligned} \tag{5}$$

Here N_{el} is the total number of elements, $\mathcal{A}_{e=1}^{N_{el}}$ is the assembly operator, and $\boldsymbol{g}^e$, $\boldsymbol{p}^e$, $\boldsymbol{r}^e$ and $\boldsymbol{q}^e$ are the element matrices and vectors corresponding to the global matrices and vectors $\boldsymbol{G}$, $\boldsymbol{P}$, $\boldsymbol{R}$ and $\boldsymbol{Q}$. The expressions for these element matrices and vectors are:

$$g_{ab}^e = \int_{\Omega^e} N_a\, \rho c\, N_b\, ds \tag{6}$$

$$p_{ab}^e = \int_{\Omega^e} N_a'\, k\, N_b'\, ds \tag{7}$$

$$r_a^e = \int_{\Omega^e} N_a\, C_R \left(\sum_{b=1}^{N_{en}} T_b(t) N_b(s) \right)^4 ds \tag{8}$$

$$q_a^e = \int_{\Omega^e} N_a q\, ds\ . \tag{9}$$

The semi-discrete system of ordinary differential equations in time, (4), has now to be solved. We solve it by using a spectral method described in the next section.

Having solved the thermal problem and obtained the temperature distribution in the truss, we now move to consider the linear thermoelastic analysis based on this temperature distribution. In doing so we actually neglect the coupling between the temperatures and the strains. More precisely, the strain field is assumed not to affect the temperature field. The governing equations in each truss member Ω_m are

$$\rho A \ddot{u} = \sigma'\ , \tag{10}$$

$$\sigma = EA\left[u' - \alpha(\mathcal{T}^h - T_{ref})\right]\ . \tag{11}$$

Here u is the axial displacement, σ is the axial stress, ρ is the mass density, E is Young's modulus, A is the cross-sectional area of the member, $\mathcal{T}^h$ is the temperature field found in the preceding thermal analysis (cf. (3)), T_{ref} is a reference temperature in which the truss is undeformed, and α is the coefficient of thermal expansion. In many cases the inertia term in the left side of (10) can be neglected, but for the sake of generality it will be maintained. In addition to (10)-(11), some boundary conditions may be applied at the joints. Also, the periodicity in time may sometimes originate from the spinning of the truss with angular velocity ω around a certain axis, say the z axis of the global Cartesian system of coordinates (x, y, z). Then a centrifugal force $f_{cen} = \rho A \omega^2 r$ (where $r = (x^2 + y^2)^{1/2}$) is present. In order to include the centrifugal effect in the model, f_{cen} is integrated along each member using the finite element shape functions as weighting functions, and the resulting concentrated forces at the nodes are applied.

In the finite element scheme, exactly the same mesh is used as in the thermal analysis. Then the semi-discrete system of equations are obtained:

$$\boldsymbol{M}\ddot{\boldsymbol{d}} + \boldsymbol{K}\boldsymbol{d} = \boldsymbol{F}\ . \tag{12}$$

$\boldsymbol{M}$ is the mass matrix, $\boldsymbol{K}$ is the stiffness matrix, $\boldsymbol{F}$ is the load vector, and $\boldsymbol{d}$ is the displacement vector, which contains the unknown displacements at the nodes in the directions x, y and z. Theses matrices and vector are obtained by

$$\boldsymbol{M} = \mathcal{A}_{e=1}^{N_{el}} \boldsymbol{m}^e; \qquad \boldsymbol{K} = \mathcal{A}_{e=1}^{N_{el}} \boldsymbol{k}^e; \qquad \boldsymbol{F} = \mathcal{A}_{e=1}^{N_{el}} \boldsymbol{f}^e \tag{13}$$

$$\boldsymbol{m}^e = [m_{aibj}^e]; \qquad \boldsymbol{k}^e = [k_{aibj}^e]; \qquad \boldsymbol{f}^e = \{f_{ai}^e\}\ . \tag{14}$$

In (13), the element matrices $\boldsymbol{m}^e$ and $\boldsymbol{k}^e$ and the element vector $\boldsymbol{f}^e$ correspond to the global matrices $\boldsymbol{M}$, $\boldsymbol{K}$ and to the global vector $\boldsymbol{F}$. In (14), the indices ai and bj correspond to degree of freedom i at node a and to degree of freedom j at node b ($i, j = 1, 2, 3$ corresponding to x, y and z). The element matrices and vector are given by:

$$m_{aibj}^e = \delta_{ij} \int_{\Omega^e} N_a\, \rho A\, N_b\, ds \tag{15}$$

$$k_{aibj}^e = \beta_i \beta_j \int_{\Omega^e} N_a'\, EA\, N_b'\, ds \tag{16}$$

$$f_{ai}^e = \beta_i \int_{\Omega^e} N_a'\, EA\alpha(\mathcal{T}^h - T_{ref})\, ds + \gamma_{ai} \int_{\Omega^e} N_a f_{cen}\, ds\ . \tag{17}$$

Here δ_{ij} is the Kronecker delta, β_i is the i direction-cosine of the element, and γ_{ai} is the i direction-cosine of the radial

vector $\boldsymbol{r} = (x, y)$ pointing to node a. In (17), the first term is due to the thermal loading and the second term is due to the centrifugal loading. If the truss moves without spinning, this second term must be omitted.

Solution of the Semi-Discrete Equations

We now show how to solve the semi-discrete systems (4) and (12) using a spectral method. Let M_T and M_d be the number of equations in (4) and (12), respectively. In both cases, periodic solutions with period $2\pi/\omega$ are sought.

We introduce the operator $\mathcal{H}$ which will be called the *harmonic operator*. It is defined as

$$\mathcal{H}(f_0, \{f_{cn}\}, \{f_{sn}\}; \psi) = f_0 + \sum_{n=1}^{\infty} (f_{cn} \cos n\psi + f_{sn} \sin n\psi). \tag{18}$$

Here f_0 is a real number, $\{f_{cn}\}$ and $\{f_{sn}\}$ are infinite-dimensional vectors, and ψ is a nondimensional time or azimuth angle, $\psi = \omega t$. We also define the operator $\mathcal{H}_N$, obtained by truncating the sum in (18) after N terms:

$$\mathcal{H}_N(f_0, \{f_{cn}\}, \{f_{sn}\}; \psi) = f_0 + \sum_{n=1}^{N} (f_{cn} \cos n\psi + f_{sn} \sin n\psi). \tag{19}$$

Now any periodic function f may be expressed via its Fourier coefficients, i.e.

$$f = \mathcal{H}(f_0, \{f_{cn}\}, \{f_{sn}\}), \tag{20}$$

and can be approximated by

$$f \simeq \mathcal{H}_N(f_0, \{f_{cn}\}, \{f_{sn}\}). \tag{21}$$

Here the dependence on ψ is omitted.

Based on these definitions, it is possible to obtain expressions for the derivative of a function expanded via the harmonic operator, and for the sum and the product of two such functions. For example, if $f = \mathcal{H}(f_0, \{f_{cn}\}, \{f_{sn}\})$, $g = \mathcal{H}(g_0, \{g_{cn}\}, \{g_{sn}\})$ and a and b are real constants, then

$$af + bg = \mathcal{H}(af_0 + bg_0, a\{f_{cn}\} + b\{g_{cn}\}, a\{f_{sn}\} + b\{g_{sn}\}). \tag{22}$$

Expressions for the Fourier coefficients of the product fg tend to be quite complex. However, if one truncates the series representing f, g and fg after a finite number of terms, N, one may use a symbolic manipulation software to obtain the formulae (see Rand and Givoli [5] and Rand [6]).

Now (21) is used to describe T^k, R^k, Q^k, d^k and F^k, the k entries of $\boldsymbol{T}$, $\boldsymbol{R}$, $\boldsymbol{Q}$, $\boldsymbol{d}$ and $\boldsymbol{F}$ in (4) and (12):

$$\begin{aligned} T^k &= \mathcal{H}_N(T_0^k, \{T_{cn}^k\}, \{T_{sn}^k\}) \quad ; \\ R^k &= \mathcal{H}_N(R_0^k, \{R_{cn}^k\}, \{R_{sn}^k\}) \quad ; \\ Q^k &= \mathcal{H}_N(Q_0^k, \{Q_{cn}^k\}, \{Q_{sn}^k\}) \quad ; \\ d^k &= \mathcal{H}_N(d_0^k, \{d_{cn}^k\}, \{d_{sn}^k\}) \quad ; \\ F^k &= \mathcal{H}_N(F_0^k, \{F_{cn}^k\}, \{F_{sn}^k\}) \end{aligned} \tag{23, 24}$$

From (23)–(24), and using $\frac{\partial^j}{\partial t^j} = \omega^j \frac{\partial^j}{\partial \psi^j}$, the kth equation in the systems (4) and (12) may be written as

$$Z_T^k = \sum_{m=1}^{M_T} \omega G_{km} \mathcal{H}_N(0, \{nT_{sn}^m\}, \{-nT_{cn}^m\})$$

$$+ P_{km} \mathcal{H}_N(T_0^m, \{T_{cn}^m\}, \{T_{sn}^m\}) + R^k - Q^k = 0 \tag{25}$$

$$Z_d^k = \sum_{m=1}^{M_d} \omega^2 M_{km} \mathcal{H}_N(0, \{-n^2 d_{cn}^m\}, \{-n^2 d_{sn}^m\})$$

$$+ K_{km} \mathcal{H}_N(d_0^m, \{d_{cn}^m\}, \{d_{sn}^m\}) - F^k = 0 \, . \tag{26}$$

The residuals Z_T^k and Z_d^k can also be expressed as

$$Z_T^k = \mathcal{H}_N(Z_{T0}^k, \{Z_{Tcn}^k\}, \{Z_{Tsn}^k\}) \, , \tag{27}$$

$$Z_d^k = \mathcal{H}_N(Z_{d0}^k, \{Z_{d\,cn}^k\}, \{Z_{d\,sn}^k\}) \, . \tag{28}$$

Since from (25) and (26), Z_T^k and Z_d^k must vanish at all times, all their Fourier coefficients must vanish identically. Consequently, each of the equations (25) and (26) is replaced by $2N + 1$ algebraic equations. The equations associated with (25) are nonlinear, while those associated with (26) are linear. Altogether, (4) yields $M_T(2N + 1)$ equations with the unknowns T_0^k, T_{cn}^k and T_{sn}^k, while (12) yields $M_d(2N+1)$ equations with the unknowns d_0^k, d_{cn}^k and d_{sn}^k.

Exploitation of Symmetry

Concentrating first on the thermal analysis, we note that many geometrical configurations of space structures possess a certain kind of symmetry, which will be defined as follows. Suppose that the total set of finite element nodes may be divided into a number of subsets, each subset having what may be termed "delayed equivalence" among its members. This means that any two nodes i and j belonging to the same subset have the same temperature with a constant time delay between them. In other words, if $T_i(t)$ and $T_j(t)$ are the temperatures of nodes i and j respectively, then $T_i(t) = T_j(t - \tau_{ij})$, where τ_{ij} is a constant time delay depending on i and j. In terms of the azimuth angle ψ, there is a constant phase shift between the two nodes: $T_i(\psi) = T_j(\psi - \Delta\psi_{ij})$, where $\Delta\psi_{ij}$ is the constant difference in phase between nodes i and j.

It is easy to see that this type of symmetry may be exploited in the present method, since phase shift constants are simply translated into multiplying factors in the final system of equations (e.g. $\sin n(\psi + \Delta\psi_{ij}) = (\cos n\Delta\psi_{ij}) \sin n\psi + (\sin n\Delta\psi_{ij}) \cos n\psi)$). All the unknowns associated with a certain node can be expressed in terms of the corresponding unknowns associated with the representative node of the same group. Doing this may lead to a significant reduction in computational cost and in re-

quired storage. It is important to note that the solution method used here, which incorporates Fourier decomposition in time, is especially appropriate for taking advantage of this type of symmetry, while other methods, such as implicit time-integration, are not capable of treating such symmetry with comparable simplicity.

A similar technique can be applied in the elastic analysis as well. One should note, however, that in the elastic case the degrees of freedom, not the nodes, have phase shift relations between them. These relations involve vector transformation between the displacements in the fixed global coordinate system and the displacements expressed in a local coordinate system rotating with the structure.

Numerical Example

The model chosen to demonstrate the method is that of a cylindrically shaped space structure made of a composite graphite-epoxy material and spinning around its axis, as shown in Figure 1. The two ends of the cylinder are assumed to be fixed to rigid bases, so that they are constrained to rotate without deformation. The thermal and mechanical properties of graphite-epoxy are: $\rho c = 1.76 \cdot 10^6$ J/m^3 °K, $k = 10.1$ W/m °K, $C_R = 9.1 \cdot 10^{-7}$ W/m^3 °K^4, $\alpha_s = 0.92$, $\rho A = 51.3$ kg/m, $EA = 1.41 \cdot 10^6$ N, $\alpha = 7.3 \cdot 10^{-7}$ 1/°K. Other parameters are $q_{\text{sun}} = 1300$ W/m^2, $T_{ref} = 299$°K, and $p/A = 20$ 1/m. The cylinder is of length 6m and radius 1.4m. Each truss member is represented by one finite element with linear shape functions.

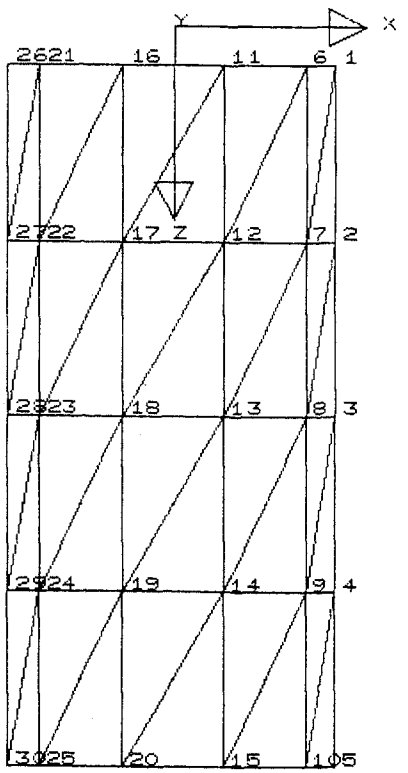

Figure 1. The cylindrically shaped space structure model.

Although the structure contains 50 joints, the temperatures at only three of them are independent unknowns, since the rest of the nodes are equivalent to one of these three in the sense of "delayed equivalence" explained previously. In the present model, nodes 1, 2 and 3 in Figure 1 were chosen as representative nodes.

The thermal analysis is considered first. The structure is assumed to be covered with an opaque material, so self-shadowing effects are present. The angular speed is set to $\omega = 10^{-5}$ rad/sec, namely the structure rotates very slowly. As a preceeding step, in order to determine the minimal number of harmonics needed in the temporal Fourier decomposition, the analysis was performed repeatedly with a different number of harmonics. convergence has been practically achieved with 12 harmonics, whereas for a smaller number of harmonics the solution obtained was quite inaccurate. For this reason, all the numerical simulations described below have been performed with 12 harmonics.

In Figure 2, the temperature at the three representative nodes as a function of the azimuth angle (or time) is shown. The figure shows that the temperature in the unshaded region is 400°K, whereas it reaches a minimum value of about 100°K in the shaded region. Thus, with an angular velocity of $\omega = 10^{-5}$ rad/sec the temperature is undergoing large variations in time and in the spatial circumferential direction. On the other hand, it is clear that the variation of temperature along the axial direction z (which manifests itself in the difference between the temperatures at nodes 1, 2 and 3) is small.

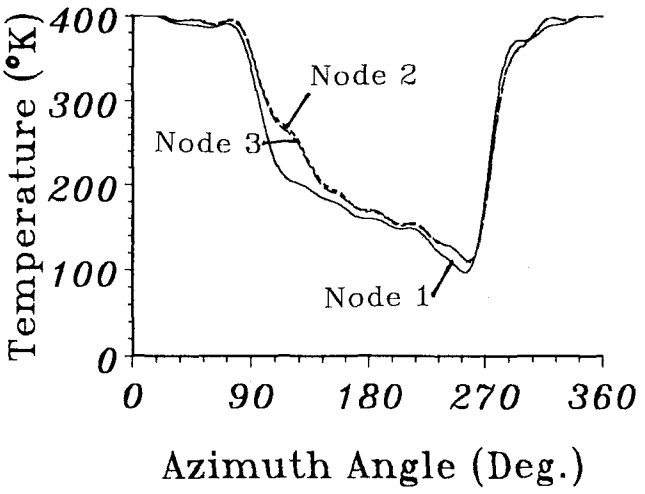

Figure 2. The temperature at the three representative nodes as a function of the azimuth angle, with an angular speed of 10^{-5} rad/sec.

The thermal analysis is now repeated with higher and lower values of ω. It turns out that the temperature distribution of Figure 2 remains unchanged when ω is decreased, and in fact the same solution is practically obtained for the quasi-staedy state $\omega = 0$. On the other hand, increasing ω above the value of 10^{-5} rad/sec makes the variations in the temperature field smaller. When the angular speed is $\omega = 10^{-3}$ rad/sec, the temperature becomes almost con-

stant (330°K). This can be regarded as the "fully dynamic" state; the structure spins so fast that no significant temperature differences develop between the shaded and unshaded regions.

Additional numerical results show that the transition from the quasi-steady state to a fully dynamic state occurs around $\omega = 10^{-4}$ rad/sec. The small value of this angular velocity means that special care must be taken when making the assumption of a quasi-steady motion, because even for a very slowly rotating structure this assumption might be inappropriate.

Now we turn to the thermoelastic analysis of the structure, based on the temperature field just found. The delayed-equivalence symmetry is exploited here as well. Since there are three degrees of freedom per node and due to the prescribed boundary conditions, there are 9 equivalence groups (excluding the group of degrees of freedom on the fixed boundaries). Using 12 harmonics in the Fourier decomposition, this means that there are only 225 unknowns out of the 2250 unknowns that one would have if symmetry was not taken advantage of. This obviously leads to great saving in computational effort and storage requirements.

We consider the case where the structure rotates with $\omega = 10^{-5}$ rad/sec. Figure 3 shows the deformed mesh at time $t = 0$ (which is identical to the deformation at times $t = 2\pi/\omega$, $t = 4\pi/\omega$, etc., due to the periodicity of the motion). The displacements are magnified by a factor of 200. The self-shadowing effect is apparent in the figure: the part of the structure exposed to solar radiation at time $t = 0$ expands much more than the shaded part of the structure, which gives rise to the unsymmetrical deformation obserevd.

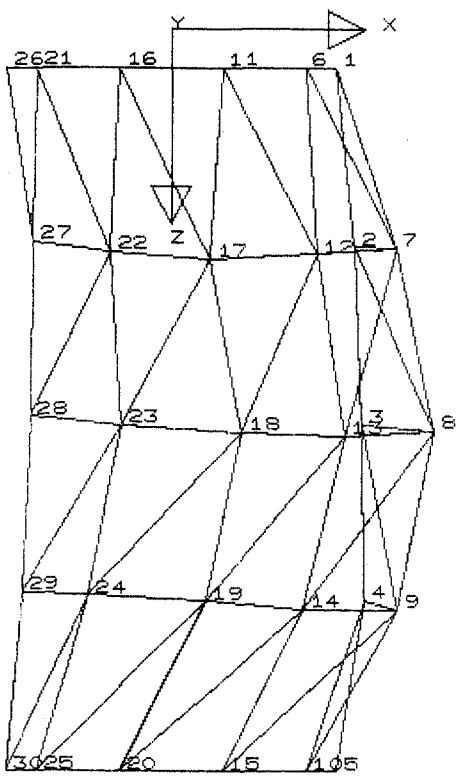

Figure 3. The deformed structure at time $t = 0$, with a scaling factor of 200.

The elastic analysis was repeated while neglecting the inertial term $\rho A\ddot{u}$ in (10). This produced practically the same results as before, which implies that the elastic problem can be regarded as quasi-steady. The same was found to be true for much higher angular speeds. A simple analytical model of a single rod may verify this fact, and demonstrate that the typical angular speed at the transition between the quasi-steady and fully-dynamic cases, is about 8 order of magnitudes larger than the one obtained in the thermal analysis. Therefore, for all practical angular speeds the motion can always be regarded as quasi-steady as far as the elastic analysis is concerend.

Acknowledgments

This work was supported in part by the L. Kraus Research Fund, V.P.R. Fund no. 160-613.

References

1. W.A. Nash and T.J. Lardner, "Parametric Investigation of Factors Influencing the Mechanical Behavior of Large Space Structures," AFOSR report no. TR-86-0858, 1985.

2. S.C. Peskett and D.T. Gethin, "Thermal Analysis of Spacecraft," Numerical Methods in Thermal Problems, eds. R.W. Lewis and K. Morgan, Vol. VI, part 1, 713–729, Pineridge Press, 1989.

3. J.D. Lutz, D.H. Allen and W.E. Haisler, "Finite Element Model for the Thermoelastic Analysis of Large Composite Space Structures," J. Spacecraft, 24, 430–436 (1987).

4. E.A. Thornton and D.B. Paul, "Thermal-Structural Analysis of Large Space Structures: An Assessment of Recent Advances," J. Spacecraft and Rockets, 22, 385–393 (1985).

5. O. Rand and D. Givoli, "A Finite Element Spectral Method With Application to the Thermoelastic Analysis of Space Structures," to appear in Int. J. Num. Meth. Engrg.

6. O. Rand, "Harmonic Variables — A New Approach to Nonlinear Periodic Problems," J. Comp. and Math. with Appl., 15, 953–961 (1988).